The hydrate structure at the end of the simulation is a mixture of sI and sII motifs (Fig. 4 and fig. S4). Despite the thermodynamic preference for sI, the coexistence of the two major types of structures for typical sI hydrate guests is well documented experimentally (30–32). Furthermore, configurations containing face-sharing 5^{12} cages have been observed in previous attempts to simulate methane hydrate nucleation and growth (17, 20) and are observed in our simulations. Because 5^{12} cages present the smallest deviation from tetrahedrality of all hydrate cavities (1), it is reasonable that these cages would predominate in the initial structure and that they would share their pentagonal faces. Additionally, sII hydrate contains more 5^{12} cages per unit cell than sI by a factor of 8. For the aforementioned reasons, it is understandable that traces of sII would form in the initial stages of sI methane hydrate nucleation. Remarkable, though, is the cooperation between the sI and sII motifs via $5^{12}6^3$ cages; these uncommon cages appear to form as a link to facilitate growth of the thermodynamically preferred sI phase from the kinetically preferred sII phase formed initially (28).

One of the most intriguing results observed from the simulations is the unforeseen molecular order of the adsorbed methane molecules in the bowl-like arrangement immediately before hydrate formation and the minuscule nucleus size needed to initiate hydrate growth; clearly the relative positions of the guest molecules, and not only the nucleus size, have bearing on the control of hydrate nucleation. The mechanism described may reflect the high methane concentration in the water phase that developed spontaneously upon quenching. Nonetheless, because the system naturally evolved from equilibrated liquid and vapor to the experimentally observed coexistence of sI and sII cages, a molecular description of these simulation trajectories aids the understanding of the hydrate nucleation process. The immediate implications from these results are that the nucleation of hydrates is more complex than previously thought, involving cooperativity between methane and water, and that hydrate nucleation must be investigated over time scales considerably longer than those of most conventional simulation studies.

References and Notes

1. E. D. Sloan, C. A. Koh, *Clathrate Hydrates of Natural Gases* (CRC Press, Boca Raton, FL, 2008).
2. K. Kaiho et al., *Paleoceanography* **11**, 447 (1996).
3. Y. Park et al., *Proc. Natl. Acad. Sci. U.S.A.* **103**, 12690 (2006).
4. E. D. Sloan, *Nature* **426**, 353 (2003).
5. L. J. Florusse et al., *Science* **306**, 469 (2004).
6. W. L. Mao et al., *Science* **297**, 2247 (2002).
7. T. Ogawa et al., *Appl. Therm. Eng.* **26**, 2157 (2006).
8. V. M. Vorotyntsev, V. M. Malyshev, P. G. Taraburov, G. M. Mochalov, *Theor. Found. Chem. Eng.* **35**, 513 (2001).
9. C. R. Fisher et al., *Naturwissenschaften* **87**, 184 (2000).
10. D. J. Milton, *Science* **183**, 654 (1974).
11. M. R. Walsh et al., *J. Energy Econ.* **31**, 815 (2009).
12. R. Boswell, *Science* **325**, 957 (2009).
13. C. A. Koh, J. L. Savidge, C. C. Tang, *J. Phys. Chem.* **100**, 6412 (1996).
14. C. A. Koh, R. P. Wisbey, X. Wu, R. E. Westacott, A. K. Soper, *J. Chem. Phys.* **113**, 6390 (2000).
15. P. M. Rodger, T. R. Forester, W. Smith, *Fluid Phase Equilib.* **116**, 326 (1996).
16. L. A. Baez, P. Clancy, *Ann. N.Y. Acad. Sci.* **715**, 177 (1994).
17. C. Moon, P. C. Taylor, P. M. Rodger, *J. Am. Chem. Soc.* **125**, 4706 (2003).
18. H. Nada, *J. Phys. Chem.* **110**, 16526 (2006).
19. J. Vatamanu, P. G. Kusalik, *J. Phys. Chem.* **110**, 15896 (2006).
20. C. Moon, P. C. Taylor, P. M. Rodger, *Faraday Discuss.* **136**, 367 (2007).
21. J. Zhang et al., *J. Phys. Chem. B* **112**, 10608 (2008).
22. Note that the time required for nucleation is volume-dependent, and induction times in simulations have no meaning unless a volume is specified. The system size reported here is comparable to previous similar studies in the literature, and thus it was necessary to extend the simulations several orders of magnitude in time to achieve nucleation.
23. See supporting material on *Science* Online.
24. M. Matsumoto, S. Salto, I. Ohmine, *Nature* **416**, 409 (2002).
25. P. Attard, M. P. Moody, J. W. G. Tyrell, *Physica A* **314**, 696 (2002).
26. E. A. Mastny, C. A. Miller, J. J. D. Pablo, *J. Chem. Phys.* **129**, 034701 (2008).
27. G. J. Guo, Y.-G. Zhang, H. Liu, *J. Phys. Chem. C* **111**, 2595 (2007).
28. J. Vatamanu, P. G. Kusalik, *J. Am. Chem. Soc.* **128**, 15588 (2006).
29. L. C. Jacobson, W. Hujo, V. Molinero, *J. Phys. Chem. B* **113**, 10298 (2009).
30. J. M. Schicks, J. A. Ripmeester, *Angew. Chem. Int. Ed.* **43**, 3310 (2004).
31. F. Fleyfel, J. P. Devlin, *J. Phys. Chem.* **95**, 3811 (1991).
32. D. K. Staykova, W. F. Kuhs, A. Salamatin, T. Hansen, *J. Phys. Chem.* **107**, 10299 (2003).
33. Supported by the NSF Materials Research Science and Engineering Center (NSF-MRSEC award DMR0820518), the U.S. Department of Energy–Basic Energy Sciences (DOE-BES award DE-FG02-05ER46242), and the CSM Hydrate Consortium (which is currently sponsored by BP, Champion Technologies, Chevron, ConocoPhillips, ExxonMobil, Halliburton, Multi-Chem Group, Nalco, Petrobras, Schlumberger, Shell, SPT Group, StatoilHydro, and Total). A.K.S. and D.T.W. were supported by NSF grant CBET-0933856. The simulations were carried out on facilities at the Golden Energy Computing Organization at the Colorado School of Mines, using resources acquired with financial assistance from NSF and the National Renewable Energy Laboratory. All graphics were prepared with VMD (S8). We thank T. Kaiser, M. Robbert, P. Rensing, T. Strobel, P. Prasad, Z. Aman, and L. Zerpa for support in computing efforts, and L. Jacobson, W. Hujo, and V. Molinero for generously sharing their cage recognition code.

Aragonite Undersaturation in the Arctic Ocean: Effects of Ocean Acidification and Sea Ice Melt

Michiyo Yamamoto-Kawai,[1]* Fiona A. McLaughlin,[1] Eddy C. Carmack,[1] Shigeto Nishino,[2] Koji Shimada[2,3]

The increase in anthropogenic carbon dioxide emissions and attendant increase in ocean acidification and sea ice melt act together to decrease the saturation state of calcium carbonate in the Canada Basin of the Arctic Ocean. In 2008, surface waters were undersaturated with respect to aragonite, a relatively soluble form of calcium carbonate found in plankton and invertebrates. Undersaturation was found to be a direct consequence of the recent extensive melting of sea ice in the Canada Basin. In addition, the retreat of the ice edge well past the shelf-break has produced conditions favorable to enhanced upwelling of subsurface, aragonite-undersaturated water onto the Arctic continental shelf. Undersaturation will affect both planktonic and benthic calcifying biota and therefore the composition of the Arctic ecosystem.

The increased rate of anthropogenic carbon dioxide (CO_2) released to the atmosphere in the 20th century has contributed to global warming and climate change because of the greenhouse effect (1). Because approximately one third of the CO_2 released has been absorbed by oceans, they are becoming more acidic (2, 3). The uptake of CO_2 by seawater increases the concentration of hydrogen ions, which lowers pH and, in changing the chemical equilibrium of the inorganic carbon system, reduces the concentration of carbonate ions (CO_3^{2-}). Carbonate ions are required by marine calcifying organisms such as plankton, shellfish, and fish to produce calcium carbonate ($CaCO_3$) shells and skeletons. Therefore, the effects of decreased CO_3^{2-} concentrations on marine organisms may place some species at risk (3, 4). For either aragonite or calcite, the two types of $CaCO_3$ produced by marine organisms, the saturation state of $CaCO_3$

[1]Department of Fisheries and Oceans, Institute of Ocean Sciences, 9860 West Saanich Road, Sidney, British Columbia V8L 4B2, Canada. [2]Research Institute for Global Change, Japan Agency for Marine-Earth Science and Technology, 2-15 Natsushima, Yokosuka, Kanagawa 237-0061, Japan. [3]Tokyo University of Marine Science and Technology, 4-5-7, Konan, Minato-ku, Tokyo 108-8477, Japan.

*To whom correspondence should be addressed. E-mail: michiyo.kawai@dfo-mpo.gc.ca

(Ω) is expressed by the product of the concentrations of CO_3^{2-} and Ca^{2+} in seawater relative to the stoichiometric solubility product at a given temperature, salinity, and pressure. Waters with $\Omega > 1$ are favorable to forming $CaCO_3$ shells and skeletons, but waters with $\Omega < 1$ are corrosive, and in the absence of protective mechanisms, dissolution of $CaCO_3$ will commence. In surface waters, Ω is lower in high-latitude oceans than tropical or temperate oceans (*4*, *5*) because colder water absorbs more CO_2 and this reduces CO_3^{2-}. Therefore, apart from intermittent upwelling of undersaturated subsurface water as observed along the North American coast (*6*), surface waters are expected to become undersaturated ($\Omega < 1$) first in high-latitude oceans as atmospheric CO_2 concentrations increase. The Southern Ocean is predicted to become undersaturated with respect to aragonite-type $CaCO_3$ (aragonite is more soluble than calcite) by 2030 (*7*) and the North Pacific by 2100 (*8*). Model simulations of the Arctic Ocean predict Ω will decrease because of freshening and increased carbon uptake as a result of sea ice retreat and that Arctic surface waters will become undersaturated with aragonite within a decade (*9*).

In the Arctic Ocean, the decrease in the summer extent of Arctic sea ice has accelerated during the 2000s (*10*, *11*). Our data show that surface waters in the Canada Basin have freshened from 1997 to 2008 (fig. S1), and oxygen isotope tracer methods have shown that the major source of this additional freshwater is sea ice meltwater (Fig. 1A) (*12*, *13*). In 2008, total alkalinity (TA) and dissolved inorganic carbon (DIC) were analyzed in surface waters to calculate Ω aragonite (*13*). Compared with observations in 1997 (*14*), Ω aragonite was significantly lower in 2008, and undersaturated waters were found in the same region

marked by low-salinity (S) and high–sea ice meltwater (Fig. 1A). Because meltwater has much lower concentrations of TA and DIC (~300 μmol kg^{-1}) than that of seawater (~2300 μmol kg^{-1}) (fig. S2) (*15*, *16*), mixing with sea ice meltwater decreases not only S but also TA and DIC. Altogether, decreases in S, TA, and DIC diminish concentrations of CO_3^{2-} and, therefore, Ω (fig. S2). Although mixing with river water also dilutes seawater, river water has higher TA and DIC (~1000 μmol kg^{-1}) than that of meltwater (*15*). Therefore, the decrease in TA, DIC, and Ω is greater when the freshwater source is sea ice meltwater rather than river water (fig. S2). The Ω aragonite values are well correlated with both the fraction of sea ice meltwater [correlation factor (r) = –0.87] (Fig. 1B) and TA (r = 0.84) and less well correlated with S (r = 0.61). This indicates that the undersaturation of surface waters is a direct consequence of the recent and substantial increase in admixture of meltwater into the surface layer.

Furthermore, because sea ice limits air-sea gas exchange, the disappearance of sea ice in summer enhances CO_2 exchange between the ocean and atmosphere. Surface partial pressure of CO_2 (P_{CO_2}) is lower in the Arctic Ocean than in the atmosphere (*17*, *18*) because of intense cooling, mixing with freshwater, and photosynthesis in summer, and, therefore, ice-free conditions increase CO_2 uptake and decrease Ω. A comparison between the 1997 (*14*) and 2008 mean profiles of Ω aragonite in the Canada Basin shows that Ω aragonite has decreased in the top 50 m (Fig. 1C), the depth of the winter mixed layer. This is the layer in which rapid uptake of CO_2 occurs and increased freshwater inputs are found.

Models indicate sea ice will continue to decrease and predict that the Arctic Ocean may

be ice-free in summer by the year 2030 (*19*). Thus, the amount of sea ice meltwater will probably continue to increase in the Canada Basin. An earlier onset of seasonal sea ice melt, together with global warming, will cause an increase in surface water temperature that will in turn act to increase Ω but to a small extent (fig. S2). Responses of phytoplankton to such changes are difficult to predict. Increased light availability and temperature may enhance photosynthesis during summer (which increases Ω by reducing seawater CO_2), but increased stratification of the seasonal layer by freshening and warming may decrease photosynthesis by blocking the resupply of nutrients from below. Nevertheless, it is clear that the melting of sea ice in the Arctic Ocean has indeed lowered Ω aragonite in the surface water to <1, and the Canada Basin is the first deep ocean where such surface undersaturation has been observed. We expect Ω will continue to decrease until the multiyear ice melts completely. Surface waters in the Canada Basin will exit the Arctic Ocean within ~10 years (*20*) and thus may contribute to a decrease in Ω in northern North Atlantic waters.

Moreover, as shown in Fig. 1C, waters with Ω aragonite of <1 are found at 100 to 200 m in the Canada Basin (*14*). The origin of this layer is Pacific water (fig. S3) that has been modified in winter on the highly productive Bering and Chukchi shelves (*21*). The characteristics of this so-called Pacific winter water (PWW) are cold temperatures (<–1°C), high nutrient concentrations, high content of CO_2 from the remineralization of organic matter, and therefore low Ω (*14*). Uptake of anthropogenic CO_2 has also influenced PWW properties. Calculations (*13*) indicate that Ω aragonite was ~1.2 during the preindustrial period when atmospheric P_{CO_2} was 280 parts per
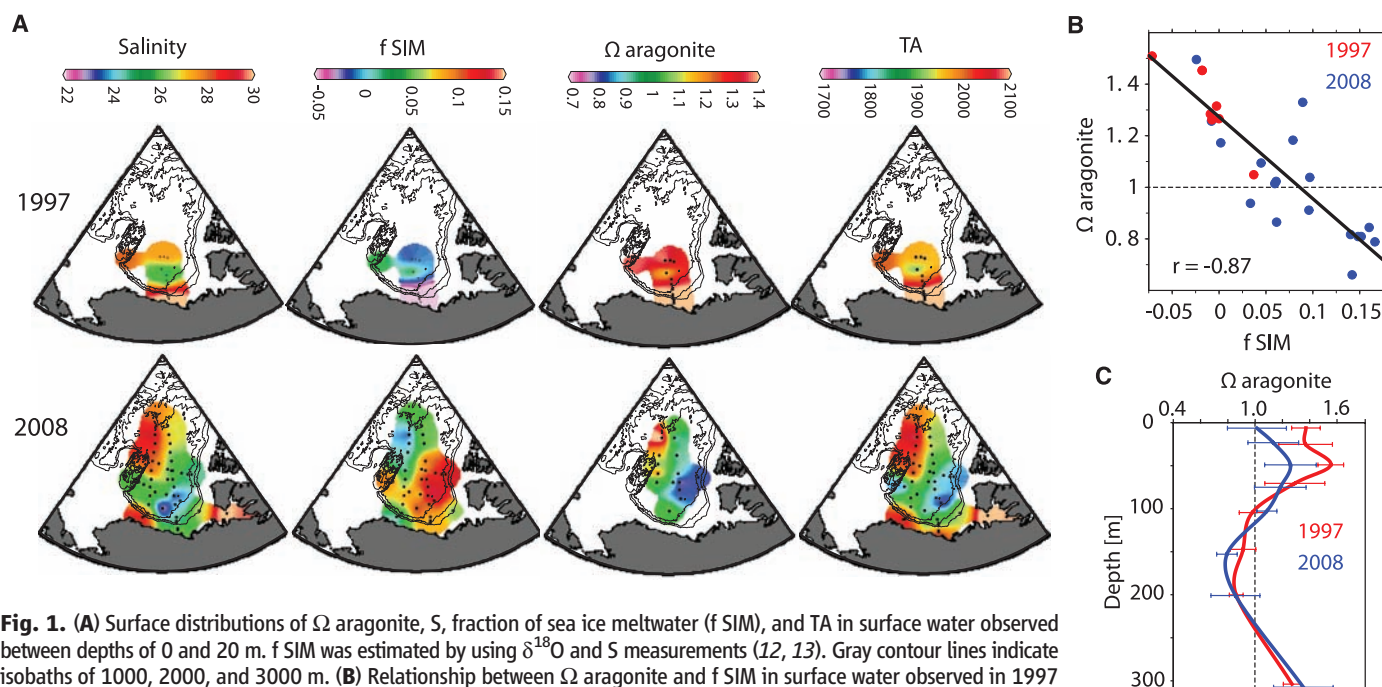

Fig. 1. (**A**) Surface distributions of Ω aragonite, S, fraction of sea ice meltwater (f SIM), and TA in surface water observed between depths of 0 and 20 m. f SIM was estimated by using $\delta^{18}O$ and S measurements (*12*, *13*). Gray contour lines indicate isobaths of 1000, 2000, and 3000 m. (**B**) Relationship between Ω aragonite and f SIM in surface water observed in 1997 (red) and 2008 (blue). (**C**) Mean vertical profile of Ω aragonite in the upper 300 m of the Canada Basin in 1997 (thick red line) (*14*) and in 2008 (thick blue line). Observations at stations where the bottom depth was >2000 m were used to calculate mean and SD (error bars) at each depth.

million (ppm) and then decreased to ~1.0 in the 1970s when atmospheric P_{CO_2} was 330 ppm. Models indicate that retreat of the ice edge past the continental shelf break will greatly enhance upwelling (*22*). In the Canada Basin, the summer ice edge has been located northward of the shelf break almost yearly since 1997 (fig. S4), and thus upwelling will bring water with Ω aragonite of <1 onto the continental shelves.

Although the possible impact of decreased Ω and undersaturation with respect to aragonite on the ecosystem is not fully understood, laboratory experiments on marine biota in an elevated CO_2 environment show that changes in Ω cause substantial changes in overall calcification rates for many species of marine organisms, including coccolithophore, foraminifera, pteropods, mussels, and clams (*4*). In the Arctic Ocean, the larvae of aragonite shell–forming pteropods *Limacina helicina* are concentrated in the top 50 m (*23*), and this is where the decrease in Ω and increase in sea ice meltwater is the most profound. Upwelling of low Ω subsurface water onto the continental shelves will also affect benthic communities, such as bivalve molluscs (*4*). Therefore, we expect that populations of both planktonic and benthic calcifying organisms in the Canada Basin are now being affected because of the rapid decrease in Ω, which is due to the melting of sea ice and upwelling. Because they are important elements of the food web, the Arctic ecosystem may be at risk and requires observation in order to predict future possible impacts on marine organisms, fisheries, and biogeochemical cycles on both regional and global scales.

References and Notes

1. Intergovernmental Panel on Climate Change, *Climate Change 2007: The Physical Science Basis; Contribution of Working Group I to the Fourth Assessment Report of the Intergovernmental Panel of Climate Change*, S. D. Solomon et al., Eds. (Cambridge Univ. Press, Cambridge, 2007).
2. C. L. Sabine et al., *Science* **305**, 367 (2004).
3. The Royal Society, "Ocean Acidification Due to Increasing Atmospheric Carbon Dioxide" (Policy Document 12/05, The Royal Society, London, 2005).
4. V. J. Fabry, B. A. Seibel, R. A. Feely, J. C. Orr, *ICES J. Mar. Sci.* **65**, 414 (2008).
5. R. M. Key et al., *Global Biogeochem. Cycles* **18**, 10.1029/2004GB002247 (2004).
6. R. A. Feely et al., *Science* **320**, 1490 (2008).
7. B. I. McNeil, R. J. Matear, *Proc. Natl. Acad. Sci. U.S.A.* **105**, 18860 (2008).
8. J. C. Orr et al., *Nature* **437**, 681 (2005).
9. M. Steinacher, F. Joos, T. L. Frölicher, G.-K. Plattner, S. C. Doney, *Biogeoscience* **6**, 515 (2009).
10. J. Stroeve, M. M. Holland, W. Meier, *Geophys. Res. Lett.* **34**, 10.1029/2007GL029703 (2007).
11. J. C. Comiso, C. L. Parkinson, R. Gersten, L. Stock, *Geophys. Res. Lett.* **35**, 10.1029/2007GL031972 (2008).
12. M. Yamamoto-Kawai et al., *J. Geophys. Res.* **114**, 10.1029/2008JC005000 (2009).
13. Materials and methods are available as supporting material on *Science* Online.
14. S. Jutterström, L. G. Anderson, *Mar. Chem.* **94**, 101 (2005).
15. L. W. Cooper et al., *Geophys. Res. Lett.* **35**, 10.1029/2008GL035007 (2008).
16. L. G. Anderson, K. Olsson, M. Chierici, *Global Biogeochem. Cycles* **12**, 455 (1998).
17. L. G. Anderson, S. Kaltin, *Polar Res.* **20**, 225 (2001).
18. N. R. Bates, S. B. Moran, D. A. Hansell, J. T. Mathis, *Geophys. Res. Lett.* **33**, 10.1029/2006GL027028 (2006).
19. J. Stroeve et al., *Eos* **89**, 13 (2008).
20. M. Yamamoto-Kawai, F. A. McLaughlin, E. C. Carmack, S. Nishino, K. Shimada, *J. Geophys. Res.* **113**, 10.1029/2006JC003858 (2008).
21. F. A. McLaughlin et al., *Deep-Sea Res.* **51**, 107 (2004).
22. E. C. Carmack, D. C. Chapman, *Geophys. Res. Lett.* **30**, 10.1029/2003GL017526 (2003).
23. H. A. Kobayashi, *Mar. Biol. (Berl.)* **26**, 295 (1974).
24. We thank A. Proshutinsky as coinvestigator of the Beaufort Gyre project and acknowledge support provided by Fisheries and Oceans Canada, the Canadian International Polar Year program, and NSF. We are grateful to S. Zimmerman and other members of the scientific teams as well as the officers and crews on the CCGS Louis S. St-Laurent. We thank M. Davelaar, A. Ross, J. McKay, and K. Tamura for their careful analyses of TA, DIC, and $\delta^{18}O$ and H. Yoshikawa, S. Noriki, N. Kurita, and T. Takamura for their help in $\delta^{18}O$ analysis.

Pleistocene Megafaunal Collapse, Novel Plant Communities, and Enhanced Fire Regimes in North America

Jacquelyn L. Gill,[1,2] John W. Williams,[1,2] Stephen T. Jackson,[3] Katherine B. Lininger,[1] Guy S. Robinson[4]

Although the North American megafaunal extinctions and the formation of novel plant communities are well-known features of the last deglaciation, the causal relationships between these phenomena are unclear. Using the dung fungus *Sporormiella* and other paleoecological proxies from Appleman Lake, Indiana, and several New York sites, we established that the megafaunal decline closely preceded enhanced fire regimes and the development of plant communities that have no modern analogs. The loss of keystone megaherbivores may thus have altered ecosystem structure and function by the release of palatable hardwoods from herbivory pressure and by fuel accumulation. Megafaunal populations collapsed from 14,800 to 13,700 years ago, well before the final extinctions and during the Bølling-Allerød warm period. Human impacts remain plausible, but the decline predates Younger Dryas cooling and the extraterrestrial impact event proposed to have occurred 12,900 years ago.

In North America, Pleistocene-Holocene deglaciation [18 to 6 thousand years ago (ka); 1 ka = 1000 calendar years ago] was marked by massive biotic upheaval, including the extinction of 34 megafaunal genera (*1*), species migration and reorganization of terrestrial communities (*2*), the rise and decline of plant communities without modern analogs (*3*), and increased biomass burning (*4*). Individualistic plant species' responses to climate change transformed the composition and distribution of vegetation formations, with rates of change highest between 13 and 10 ka (all ages are reported as calendar years before the present) (*2*). Many North American fossil pollen assemblages between 17 and 9 ka lack modern analogs, suggesting parent vegetation formations that were compositionally unlike any today (*5*). In the upper Midwest of the United States, "no-analog" pollen assemblages contained high percentages of temperate broadleaved trees, particularly *Fraxinus* (ash), *Ostrya/Carpinus* (hophornbeam/ironwood), and *Ulmus* (elm), coexisting with boreal conifers such as *Picea* (spruce) and *Larix* (larch) (*2*, *3*). These no-analog communities apparently formed in response to higher-than-present insolation and temperature seasonality, but it has been suggested that they may have been linked to the Pleistocene megafauna (*3*).

Deglaciation and vegetation turnover coincided with the end-Pleistocene megafaunal extinctions in North America, which was part of a global time-transgressive extinction wave that was taxonomically selective and more severe for species of large body size (*6*, *7*). In North America, >50% of all mammal species >32 kg and all species >1000 kg were extirpated (*1*). Hypothesized extinction drivers include climate change, human hunting, or a combination of the two; the relative importance of these mechanisms is debated (*1*, *8*). An extraterrestrial impact at 12.9 ka has also been proposed (*9*) but is disputed (*4*, *10*).

The apparent coincidence between megafaunal extinction, peak rates of vegetation change, and the rise of the no-analog communities (*3*) in eastern North America suggests causal relationships, but the direction of causation remains unclear. Hypothesized extinction mechanisms linked to vegetation change include habitat loss and fragmentation, disruption of coevolved plant and animal communities, and loss of vegetation mosaics (*1*, *8*). Conversely, the removal of keystone megaherbivores might have triggered trophic

[1]Department of Geography, University of Wisconsin, Madison, WI 53706, USA. [2]Center for Climatic Research, University of Wisconsin, Madison, WI 53706, USA. [3]Department of Botany, University of Wyoming, Laramie, WY 82071, USA. [4]Department of Natural Science, Lincoln Center Campus, Fordham University, New York, NY 10023, USA.